Goddard Grant

IN-93-CR

103724

38 P.

SPACE RADIATION LABORATORY

CALIFORNIA INSTITUTE OF TECHNOLOGY
Pasadena, California   91125

SEMI-ANNUAL STATUS REPORT

for

NATIONAL AERONAUTICS AND SPACE ADMINISTRATION
Grant NGR 05-002-160*
"RESEARCH IN PARTICLES AND FIELDS"

for

1 April 1986 - 31 March 1987

E. C. Stone, Principal Investigator
L. Davis, Jr., Coinvestigator
R. A. Mewaldt, Coinvestigator
T. A. Prince, Coinvestigator

*NASA Technical Officer: Dr. W. Vernon Jones, High Energy Astrophysics

TABLE OF CONTENTS

SEMI-ANNUAL STATUS REPORT

NASA Grant NGR 05-002-160

Space Radiation Laboratory (SRL)
California Institute of Technology

1 April 1986 - 31 March 1987

This report covers the research activities in Cosmic Rays, Gamma Rays, and Astrophysical Plasmas supported under NASA Grant NGR 05-002-160. The report is divided into sections which describe the activities, followed by a bibliography.

This group's research program is directed toward the investigation of the astrophysical aspects of cosmic rays and gamma rays and of the radiation and electromagnetic field environment of the Earth and other planets. We carry out these investigations by means of energetic particle and photon detector systems flown on spacecraft and balloons.

1. Particle Astrophysics

This research program is directed toward the investigation of galactic, solar, interplanetary, and planetary energetic particles and plasmas. The emphasis is on precision measurements with high resolution in charge, mass, and energy. The main efforts of this group, which are supported partially or fully by this grant, have been directed toward the following two categories of experiments.

1.1. Activities in Support of or in Preparation for Spacecraft Experiments

These activities generally embrace prototypes of experiments on existing or future NASA spacecraft or they complement and/or support such observations.

1.1.1. The High Energy Isotope Spectrometer Telescope (HEIST)

Over the past few years we have been developing a balloon-borne High Energy Isotope Spectrometer Telescope (HEIST) designed to make high resolution measurements of isotopes in the element range from H to Ni ($1 \leq Z \leq 28$) at energies from ~0.4 to 2.0 GeV/nucleon. The instrument, which is a collaborative effort with the Danish Space Research Institute and the University of New Hampshire, consists of a stack of 12 NaI(Tl) scintillators of total thickness 88 g/cm^2, two Cerenkov counters

(C1 and C2), and two plastic scintillators (see Figure 1). HEIST determines the mass of individual nuclei by measuring both the change in the Lorentz factor ($\Delta\gamma$) that results from traversing the NaI stack, and the energy loss (ΔE) in the stack, and is designed to achieve a typical mass resolution of 0.25 amu.

The energy range covered by HEIST can be "tuned" by choice of the index of refraction (n) of the two Cerenkov counters. In its initial configuration (HEIST-1), flown in 1984, the top counter (C1) was composed of aerogel (n=1.10), giving an energy range of ~1.5 to 2 GeV/nucleon. In its present configuration (HEIST-2) C1 is composed of Teflon (n = 1.33) and C2 is Pilot 425 (n = 1.50) and the instrument is capable of resolving isotopes from Be to Ni over the energy range from ~0.4 to ~1.1 GeV/nucleon, with both improved mass resolution and yield over the initial version of the instrument.
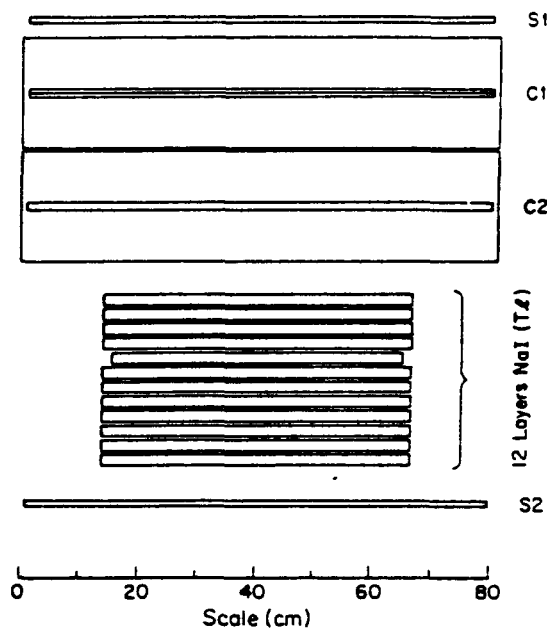

Figure 1

The new Cerenkov counters for HEIST-2, developed in collaboration with W. R. Webber of the University of New Hampshire, have significantly improved light yield, a result of considerable progress in several areas of Cerenkov counter development. In particular, improvements were made in wave-shifting and high-reflectance painting techniques, and a new Teflon "sandwich" radiator was developed that optimizes the output of C1. These developments will be reported at the Moscow International Cosmic Ray Conference. Other improvements in HEIST-2 include a commandable high-gain mode, normally used for testing with ground-level muons, that can be used in flight to provide measurements of H and He isotopes with several hundred MeV/nucleon.

HEIST-2 was readied for balloon flight during the early summer of 1986 and was shipped to Ainsworth, Nebraska where it successfully passed final preflight tests.

HEIST was launched on September 7, 1986 on a 23 x 10^6 ft^3 Winzen balloon. The instrument was turned on shortly after launch and began recording heavy nuclei. Data received indicated that all systems were operating normally and that the newly designed trigger system was successful in reducing the event background due to high energy He nuclei. Unfortunately, at an altitude of ~70,000 ft the balloon burst catastrophically. The package parachuted to earth but suffered some damage to the pressure vessel, to the top and bottom plastic scintillators, and to the top Cerenkov counter, when it was pulled over on its side upon landing. HEIST was then returned to our laboratory for repair. Repairs to the pressure vessel and scintillators are now complete; those to the Cerenkov counters are in progress. Although we had planned to re-fly HEIST-2 during the 1987 summer balloon campaign from Prince Albert, Canada, the two Australian balloon flights planned by our GRIP gamma ray experiment to image supernova 1987a have forced us to delay a reflight of HEIST until 1988.

The analysis of data from the 1984 flight of HEIST-1 is the focus of the Ph.D. thesis of J. E. Grove. Considerable effort has gone into the development and optimization of algorithms to determine the position and energy-loss of ions traversing the NaI stack and we presently achieve a position resolution of ~2mm (rms) in each layer, while the energy loss resolution of each layer is ~1% (rms). These algorithms have been used to compute trajectories and energy loss profiles for various subsets of the flight data, including nuclei from carbon to iron.

We have recently been concentrating our data analysis efforts on mapping the response of the aerogel Cerenkov counter. Because the counter is actually a mosaic of 16 segments, each of slightly different index, some care is required to match the response of the various segments. Analysis of flight data indicates that the relative response of the segments has changed somewhat from the prelaunch Bevalac calibration and we are presently using oxygen nuclei obtained during the flight to renormalize this response. We are presently attempting to normalize the response of the sixteen aerogel blocks to an accuracy of less than a few percent using a flight data set consisting of penetrating oxygen nuclei. We are also exploring the use of the Cerenkov to ionization (C/I) ratio to achieve improved velocity resolution over the use of the Cerenkov signal alone.

In addition, we have made considerable progress in isolating the various contributions to the velocity resolution of Cerenkov counters including photoelectron statistics, index of refraction variations, and fluctuations in the Cerenkov light produced by delta rays. Fits to the response measured at the Bevalac at three different beam energies give an rms variation in the index of refraction within a single aerogel block of $\sigma_n/n = 0.0003$, which would contribute ~0.1 amu to the mass resolution of ^{56}Fe nuclei, and a lesser amount to lighter elements in proportion to their mass.

Our work on HEIST has resulted in the following recent talks and papers:

- "High Resolution Cerenkov Detectors for Use in a Cosmic Ray Isotope Spectrometer ," E. R. Christian et al., *Proceedings of the 20th International Cosmic Ray Conference, Moscow, USSR* **2**, 382 (1987).

● "Cosmic Ray Isotope Measurements with a High Energy Spectrometer," E. R. Christian et al., *Proceedings of 20th International Cosmic Ray Conference, Moscow, USSR* **1**, 364 (1987).

Some of the results from one of these papers are summarized below.

High Resolution Cerenkov Detectors
for use in a Cosmic Ray Isotope Spectrometer

The High Energy Isotope Spectrometer Telescope (HEIST) uses Cerenkov counters and a stack of NaI crystals to measure charge (Z), mass (M), and kinetic energy of incident nuclei using the Cerenkov-total energy technique. The latest version of this instrument (HEIST-2) includes two Cerenkov counters, one of Teflon (index of refraction n=1.33) and a second of Pilot-425 (n=1.5). In a Cerenkov-total energy spectrometer the mass resolution is typically dominated by the uncertainty in the velocity measurement. We have modeled the various contributions to the resolution of HEIST-2 from the Teflon counter, and the results for ^{56}Fe at zenith angle $\theta = 20°$ are shown in Figure 2.
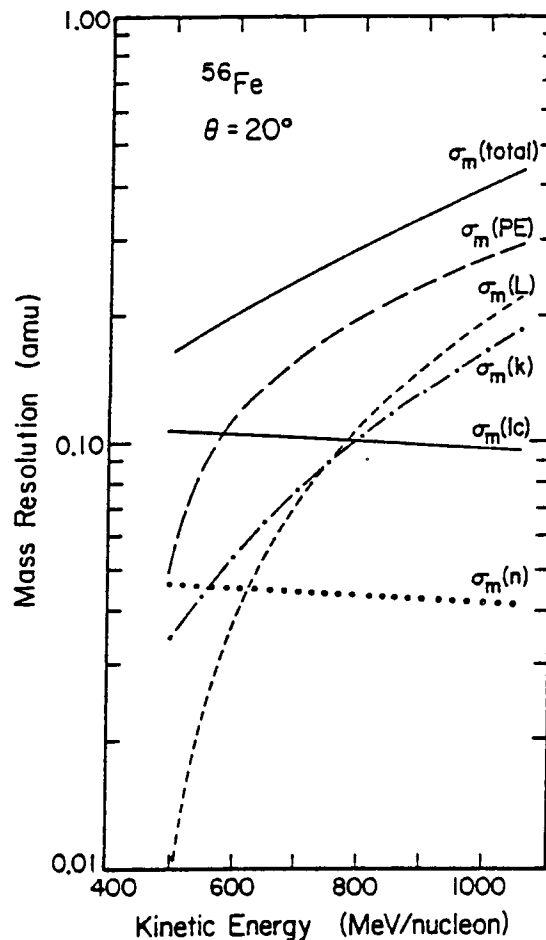

Figure 2

For large-angle particles, uncertainty in the trajectory can produce an unacceptably large mass uncertainty. We can alleviate this problem by determining velocity, not from the pathlength-corrected Cerenkov signal, but from the ratio of the Cerenkov signal to the dE/dx signal from the nearest NaI stack layer ($R \equiv C/S$). Pathlength effects are therefore removed automatically, with the only source of error the small effect of multiple Coulomb scattering in the few grams/cm^2 of radiator and NaI. However, dividing by S introduces the Landau fluctuations in the energy loss within the stack layer into the velocity measurement. We have, therefore, traded a contribution from trajectory uncertainty for a contribution from Landau fluctuations, but the latter is smaller for typical angles and reasonable angular resolution ($\sim 1°$).

Of the remaining contributions to mass uncertainty, photoelectron statistical fluctuations dominate, with the PE contribution typically about twice the Landau contribution (see Figure 2). Both are proportional to the mass to charge ratio A/Z. There is another benefit to using C/S. One can show that the mass uncertainty due to PE fluctuations $\sigma_m(PE) \propto [\, \partial R/\partial \gamma \,]^{-1}$. Since the Cerenkov signal is an increasing function of γ, and the dE/dx signal a decreasing function, determining velocity from the C/S ratio further improves mass resolution by increasing the variation of the signal with respect to the particle velocity. For example, at 750 MeV/nuc the PE contribution to the mass resolution determined from C/S is approximately 80% of that determined directly from the Cerenkov response. Also at 750 MeV/nuc and $\theta = 20°$, the sum in quadrature of the PE and Landau contributions determined from C/S is approximately 60% of the sum of PE and trajectory contributions (assuming a 1° angular resolution) determined from C alone.

Fluctuations in the number and, more importantly, the energies of knock-on electrons produced above and within the radiator also contribute to the mass error. We have calculated the knock-on Cerenkov light and its rms variation by numerical techniques, using a procedure similar to that of Lezniak. We find, again for example for ^{56}Fe at 750 MeV/nuc, that the knock-ons generate about 5.5% (with an rms variation of 0.3%) of the primary Cerenkov light at that energy. We see in Figure 2 that the knock-on contribution is non-negligible and approximately equal to the Landau contribution. Note that the knock-on contribution $\sigma_m(k) \propto A/Z$.

There are other potential contributions to mass resolution which, while not of a fundamental nature, must be carefully controlled. Variations in light-collection efficiency can be mapped either at an accelerator or in flight, but residual small-scale variations which are not removed by the maps will lead to an uncertainty in mass. In addition, while gross variations in index of refraction will masquerade as light-collection non-uniformities and be included in the maps, small-scale index variations may also lead to mass uncertainty. Figure 2 shows that a residual rms variation in light collection uniformity of $\sigma_{lc} \approx 3 \times 10^{-3}$, where the uniformity is nominally 1, is necessary to reduce this contribution to 0.1 amu for ^{56}Fe. Although to date we have no measurement of the index variation for Teflon, we have assumed here a residual rms variation of $\sigma_n \approx 3 \times 10^{-4}$, the value we determined for an aerogel radiator of index n = 1.1. Because of the differences in the methods of manufacture of aerogels vs. Teflon, we expect that σ_n will be smaller in Teflon. Both of these contributions are proportional to A but independent of Z, and therefore tend to be insignificant for lighter nuclei.

Similar velocity resolution is obtained from the Pilot-425 counter and, in the region where the useful energies of the two Cerenkov counters overlap, the final mass resolution is correspondingly improved. As a result of the Cerenkov counter developments described here, HEIST-2 should be capable of resolving a wide range of cosmic ray isotopes from Be to Ni over the energy range from ~0.4 to ~1.1 GeV/nucleon. We hope to fly the instrument from northern Canada during the summer of 1988.

In addition to our work on HEIST, we also devoted considerable effort during the past year to defining the goals and capabilities of Astromag, the proposed superconducting magnet facility for particle astrophysics on the Space Station. In particular, we have addressed the use of Astromag to measure the isotopic composition of high energy cosmic rays using the magnet/Cerenkov method, an approach that draws heavily on our experience with aerogel Cerenkov counters in HEIST. Our work on Astromag has resulted in the following recent talks and papers.

- "ASTROMAG: The Particle Astrophysics Magnet Facility", Interim Report of the Astromag Definition Team. Editors: J. F. Ormes, M. Israel, M. Wiedenbeck, and R. Mewaldt (1986).

- "ASTROMAG: A Superconducting Particle Astrophysics Magnet Facility for the Space Station", M. A. Green et al., *IEEE Transactions on Magnetics*, **23** , 1240 (1987).

- "A Particle Asrophysics Magnet Spectrometer Facility for Space Station", J. F. Ormes, M. Israel, M. Wiedenbeck, and R. Mewaldt, *Proceedings of the 20th International Cosmic Ray Conference, Moscow, USSR* **2** , 378 (1987).

1.1.2. Low Energy Isotope Spectroscopy

In April of 1986 we responded on very short notice to a request from NASA Headquarters to propose low-cost experiments that might be launched by a Scout rocket into low-Earth orbit. We proposed two possibilities: 1) The unfinished COMPAS experiment that we were developing jointly with Goddard, Maryland, MPI and New Hampshire for the US spacecraft of the ISPM (Ulysses) mission until this spacecraft was canceled in late 1981; 2) the ACE experiment described below. During the next few months we studied the first option (COMPAS) in more detail and provided additional information for a study being conducted by Goddard Space Flight Center on this and other possible low-cost missions. In February of 1987 we participated in the Small Payloads Workshop held at Goddard, which considered these and other possible Scout missions.

In the course of our study to date it has been determined that all or part of COMPAS could be accommodated by a Scout launch and available spacecraft with only minor modifications. COMPAS consists of five sensors designed to determine the isotopic and elemental composition of energetic particles from ~40 keV/nucleon to ~400 MeV/nucleon. A key element of COMPAS is the MAST telescope that was being built by our group to measure the elemental and isotopic composition of galactic

cosmic rays, the anomalous cosmic rays, and solar energetic particles. Although a low-altitude Earth-orbit is not as desirable as being outside the magnetosphere in interplanetary space, with a polar orbit MAST could provide a collecting power for the isotopes of low energy galactic cosmic rays and solar particles exceeding that of all previous experiments, and it would measure the charge state and isotopic composition of the anomalous cosmic rays.

1.2. Experiments on NASA Spacecraft

The SR&T grant program of the Space Radiation Laboratory is strengthened by and contributes to the other programs described here. Activities related to these programs are primarily funded by mission-related contracts but grant funds are used to provide a general support base and the facilities which make these programs possible.

1.2.1. An Electron/Isotope Spectrometer (EIS) Launched on IMP-7 on 22 September 1972 and on IMP-8 on 26 October 1973

This experiment is designed to measure the energy spectra of electrons and positrons (0.16 to ~6 MeV), and the differential energy spectra of the nuclear isotopes of hydrogen, helium, lithium, and beryllium (~2 to 50 MeV/nucleon). In addition, it provides measurements of the fluxes of the isotopes of carbon, nitrogen, and oxygen from ~5 to ~15 MeV/nucleon. The measurements from this experiment support studies of the origin, propagation, and solar modulation of galactic cosmic rays; the acceleration and propagation of solar flare and interplanetary particles; and the origin and transport of energetic magnetospheric particles observed in the plasma sheet, adjacent to the magnetopause, and upstream of the bow shock.

The extensive EIS data set has been utilized in comprehensive studies of solar, interplanetary, and magnetospheric processes. Correlative studies have involved data from other IMP investigations and from other spacecraft, as well as direct comparisons of EIS data from IMP-7 and IMP-8.

During the past year our studies of IMP data have resulted in the following papers:

- "^{3}He in Galactic Cosmic Rays," R. A. Mewaldt, *Ap. J.* **311**, 979 (1986).

- "A Re-Examination of the Cosmic Ray Helium Spectrum and the ^{3}He/^{4}He Ratio at High Energies ," W. R. Webber et al., *Ap.J.* **312**, 178 (1987).

- "Solar Cycle Variations of Anomalous ^{4}He as Deduced by Studies of Cosmic Ray ^{3}He," A. C. Cummings et al., *Geophys. Res. Letters.* **13**, 1043 (1986).

- "Solar Cycle Variations of Anomalous ^{4}He as Revealed by Studies of Cosmic Ray ^{3}He ," A. C. Cummings et al., *Bull. of Am. Phys. Soc.* **31**, 872 (1986).

• "Large-Scale Radial Gradient of Anomalous Cosmic-Ray Oxygen from 1 to ~ 30 AU," A. C. Cummings et al., *Proceedings of the 20th International Cosmic Ray Conference, Moscow, USSR* **3**, 425 (1987).

1.2.2. An Interstellar Cosmic Ray and Planetary Magnetospheres Experiment for the Voyager Missions Launched in 1977.

This experiment is conducted by this group in collaboration with F. B. McDonald and J. H. Trainor (Goddard Space flight Center), W. R. Webber (University of New Hampshire), and J. R. Jokipii (University of Arizona), and has been designated the Cosmic Ray Subsystem (CRS) for the Voyager Missions. The experiment is designed to measure the energy spectra, elemental and (for lighter elements) isotopic composition, and streaming patterns of cosmic-ray nuclei from H to Fe over an energy range of 0.5 to 500 MeV/nucleon and the energy spectra of electrons with 3 - 100 MeV. These measurements will be of particular importance to studies of stellar nucleosynthesis, and of the origin, acceleration, and interstellar propagation of cosmic rays. Measurements of the energy spectra and composition of energetic particles trapped in the magnetospheres of the outer planets are used to study their origin and relationship to other physical phenomena and parameters of those planets. Measurements of the intensity and directional characteristics of solar and galactic energetic particles as a function of the heliocentric distance will be used for *in situ* studies of the interplanetary medium and its boundary with the interstellar medium. Measurements of solar energetic particles are crucial to understanding solar composition and solar acceleration processes.

The CRS flight units on both Voyager spacecraft have been operating successfully since the launches on August 20, 1977 and September 5, 1977. The CRS team participated in the Voyager 1 and 2 Jupiter encounter operations in March and July 1979, in the Voyager 1 and 2 Saturn encounters in November 1980 and August 1981, and in the Voyager 2 Uranus encounter in January 1986. The Voyager data represent an immense and diverse data set, and a number of scientific problems are under analysis. These investigation topics range from the study of galactic particles to particle acceleration phenomena in the interplanetary medium to plasma/field/energetic particle interactions, to acceleration processes on the sun, to studies of elemental abundances of solar, planetary, interplanetary, and galactic energetic particles, and to studies of particle/field/satellite interactions in the magnetospheres of Jupiter, Saturn, and Uranus.

The following publications and papers for scientific meetings, based on Voyager data, were generated:

• "Energetic Charged Particles in the Uranian Magnetosphere," E. C. Stone et al., *Science* **233**, 93 (1986).

• "Evidence for a Latitudinal Gradient of the Cosmic Ray Intensity Associated with a Change in the Tilt of the Heliospheric Current Sheet," S. P. Christon et al., *Geophys. Res. Letters.* **13**, 777 (1986).

● "The Voyager 2 Encounter with the Uranian System," E. C. Stone and E. D. Miner, *Science* **233**, 39 (1986).

● "Solar Cycle Variations of Anomalous ^{4}He as Deduced by Studies of Cosmic Ray ^{3}He," A. C. Cummings et al., *Geophys. Res. Letters.* **13**, 1043 (1986).

● "Solar Cycle Variations of Anomalous ^{4}He as Revealed by Studies of Cosmic Ray ^{3}He ," A. C. Cummings et al., *Bull. of Am. Phys. Soc.* **31**, 872 (1986).

● "Latitudinal and Radial Gradients of Anomalous and Galactic Cosmic Rays in the Outer Heliosphere," A. C. Cummings et al., *Geophys. Res. Letters* **14**, 174 (1987).

● "Observation of a Large Negative Latitudinal Gradient of Anomalous Oxygen," A. C. Cummings et al., *EOS Trans. AGU Nov.* **67**, 1150 (1986).

● "The Voyager 2 Encounter with Uranus," E. C. Stone, *Bull. of the Amer. Astron. Soc.* **18**, 1006 (1986).

● "Elemental Composition of the Anomalous Cosmic-Ray Component," A. C. Cummings and E. C. Stone, *Proceedings of the 20th International Cosmic Ray Conference, Moscow, USSR* **3**, 413 (1987).

● "Radial and Latitudinal Gradients of Anomalous Cosmic-Ray Oxygen and Helium and Galactic Cosmic Rays in the Outer Heliosphere," A. C. Cummings et al., *Proceedings of the 20th International Cosmic Ray Conference, Moscow, USSR* **3**, 417 (1987).

● "Energy Spectra of Anomalous Cosmic-Ray Oxygen During 1977-1987," A. C. Cummings and E. C. Stone, *Proceedings of the 20th International Cosmic Ray Conference, Moscow, USSR* **3**, 421 (1987).

● "Large-Scale Radial Gradient of Anomalous Cosmic-Ray Oxygen from 1 to ~ 30 AU," A. C. Cummings et al., *Proceedings of the 20th International Cosmic Ray Conference, Moscow, USSR* **3**, 425 (1987).

Two of these studies are summarized here.

Composition of the Anomalous Cosmic-Ray Component

The anomalous cosmic-ray component is characterized by anomalous enhancements in the fluxes of helium, nitrogen, oxygen, and neon with energies of ~5 to ~50 MeV/nucleon. Recognition that these elements have high first ionization potentials and are therefore neutral in the local interstellar medium led to the widely held model in which anomalous cosmic rays originate as neutral interstellar atoms that drift into the heliosphere, become singly-ionized near the Sun, and are then convected outward by the solar wind to the outer heliosphere where the ions are accelerated to higher energies.

The general spectral features of the anomalous component are shown in Figure 3a, which displays the observed energy spectra of carbon, nitrogen, and oxygen for the period 1985 day 274 to 1986 day 254. Each spectrum is an unweighted average of independent spectra obtained from the CRS on Voyagers 1 and 2.

The carbon and oxygen fluxes in Figure 3a are in close agreement near 100 MeV/nuc, as is expected since the galactic cosmic-ray component, which dominates at this energy, has a C/O ratio of ∼1. The large increases in the intensity of the spectra of oxygen and nitrogen below ∼50 MeV/nuc are due to the anomalous component. The carbon spectrum has only a small increase near 10 MeV/nuc, which we ascribe to anomalous carbon at about the 1% level of oxygen. We believe that this is the first observation of anomalous carbon and is made possible because the Voyagers are far enough removed from the Sun so that the low-energy solar or interplanetary component, which dominated this energy region in previous measurements, is absent.
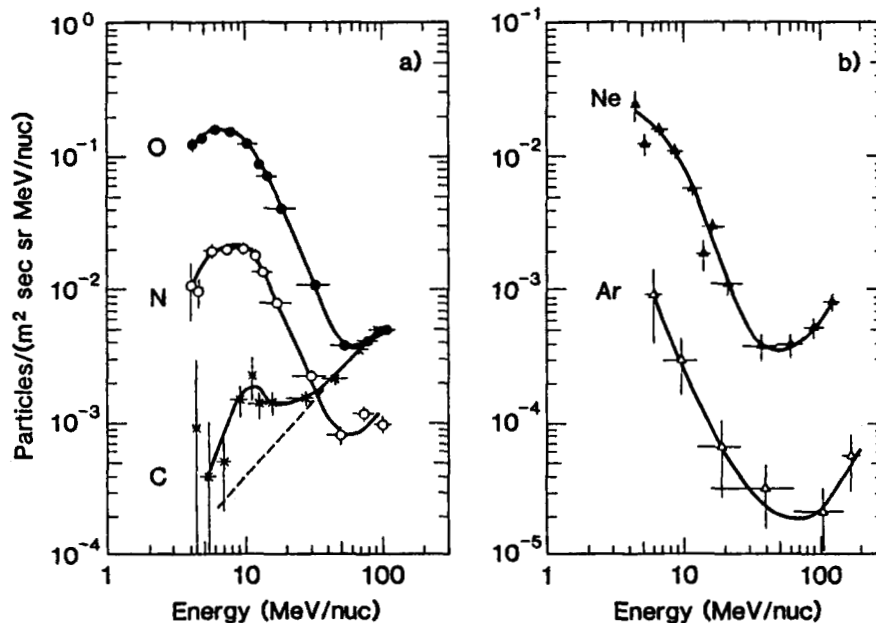

Figure 3

The Ne and Ar spectra shown in Figure 3b are also dominated by the anomalous component below ∼50 MeV/nuc. This measurement represents a confirmation of the presence of anomalous Ar.

Thus six elements are now known to comprise the anomalous component: helium, carbon, nitrogen, oxygen, neon, and argon. Assuming the model of Fisk et al. for the origin of the anomalous component, we have inferred the abundances of the inflowing neutral gas relative to oxygen from the anomalous component measurements.

We considered each step in the process of converting the neutrals into the observed spectra. The cross sections for charge exchange with the solar wind and for photoionization by solar ultraviolet radiation are reasonably well known. We calculated correction factors for these ionization processes together with estimates of their uncertainties.

In order to estimate the effect of acceleration on the observed abundances of particles with different A/Z, we used the analysis of Droge and Schlickeiser for second-order Fermi acceleration. Their approximation of first-order Fermi acceleration as a distributed process yields the same A/Z dependence. However, the parameters involved in the acceleration process are rather poorly understood. In order to gauge the uncertainty introduced in the relative abundances, we calculated two sets of acceleration correction factors by making two widely different assumptions regarding the injection mode of the particles. Therefore, in Figure 4 we show two estimates of the local interstellar medium neutral gas abundances relative to oxygen, corresponding to injection at common velocity and common momentum, respectively. Also shown are various estimates from other measurements.
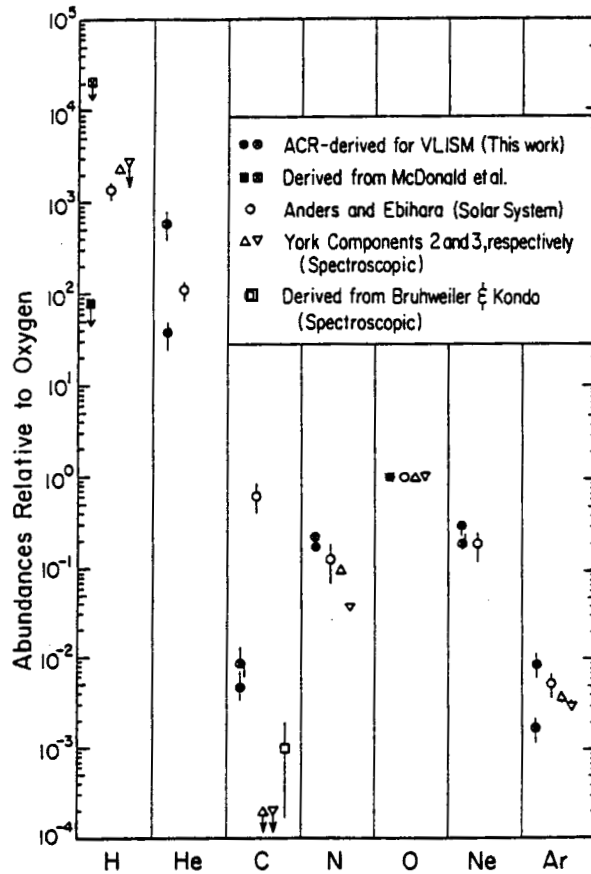

Figure 4

We find that the ratio of our estimate based on the common velocity injection mode to that based on common momentum for a particle with mass number A is proportional to $(16/A)^2$. Thus the injection assumption is not very important for elements with mass number near the reference element oxygen, e.g., nitrogen and neon. However, for elements such as hydrogen and helium the uncertainties are large enough that further work is needed before we can be confident of the neutral abundances of these elements.

For elements other than hydrogen and helium it is possible to quantitatively address some issues with the data in Figure 4. Consider first the nitrogen, oxygen, neon, and argon. These atoms all have first ionization potentials larger than that of hydrogen and might be expected to be predominantly neutral in the interstellar medium. The abundances we derive for nitrogen and neon are in excellent agreement with the Anders and Ebihara solar system abundances, indicating that there is no large depletion of these atoms in the very local interstellar medium. The abundance of argon is also in general agreement with the solar system compilation, although the derived abundance is somewhat dependent on the injection mechanism assumed.

We note that since the charge-exchange cross section for neon is much smaller than that of oxygen, the fact that Ne/O is normal suggests that significant charge-exchange processes are not occurring at the heliospheric interface, contrary to the suggestion of Fahr and Ripken. Also, our abundance of nitrogen is significantly greater than that of both components 2 and 3 of York, which have recently been proposed as being representative of the local and the very local interstellar medium, respectively.

The relative abundance we derive for carbon is a factor of ~100 below that of Anders and Ebihara. This is consistent with the expectation that most of the carbon is ionized in the interstellar medium because of its lower first ionization potential. A local spectroscopic measurement of neutral carbon was made by Bruhweiler and Kondo along a 7 parsec line of sight. Our measurement is a factor of ~5-10 higher than the rather uncertain value derived from the spectroscopic observations. Our measurement is also greater, by a factor of ~25-50, than the upper limits from the York components 2 and 3. This difference, together with the nitrogen difference noted earlier, suggests that neither of the two York components can be identified with the very local interstellar medium.

Energetic Electron Measurements in the Magnetosphere of Uranus

The Voyager 2 Cosmic Ray System (CRS) found high intensities of trapped electrons at MeV energies in the Uranian magnetosphere during the planetary encounter on January 24, 1986. The highest intensities and lowest phase space densities were found near closest approach to Uranus, indicating that the electrons may have been accelerated adiabatically as the result of inward radial transport from source populations of lower energy electrons in the outer magnetosphere and magnetotail. The radial profiles of the trapped electrons showed clear evidence of strong modulation by satellite sweeping. The lack of comparable features for MeV electrons in the Saturnian magnetosphere could be understood in terms of relatively higher electron sweeping rates in the magnetic field of Uranus. Also measured were lower intensity fluxes of trapped protons, but these measurements were severely limited by large backgrounds from the electrons. Like at Saturn, no evidence was found for significant fluxes of heavier ions within the magnetosphere of Uranus, due to the lack of an internal ion sources such as the volcanically-active satellite Io in Jupiter's inner magnetosphere.

Electron Profiles in Magnetic Coordinates. Since last year's preliminary report in *SCIENCE* the CRS data analysis has concentrated on mapping of the electron intensities in magnetic coordinates with the offset, tilted dipole (OTD) and dipole-quadrapole (Q_3) field models for Voyager measurements of the planetary magnetic field. Figure 5 shows the radial profiles of ≥ 1.1 MeV and ≥ 3.1 MeV electrons plotted as functions of magnetic L value from the Q_3 model for the inbound and outbound legs of the encounter trajectory. Also shown versus L is the corresponding spacecraft trajectory in units of B/B_0, where B is the local measured field magnitude and B_0 is the magnitude at the magnetic equator of the field on the local magnetic field line. The vertical dashed lines delimit the range of L values at which the satellites Miranda, Ariel, and Umbriel cross the magnetic equator. During their orbits around Uranus the positions of the satellites undergo large changes in L and B/B_0 due to the 60° tilt of the magnetic dipole axis with respect to the rotation axis of Uranus.
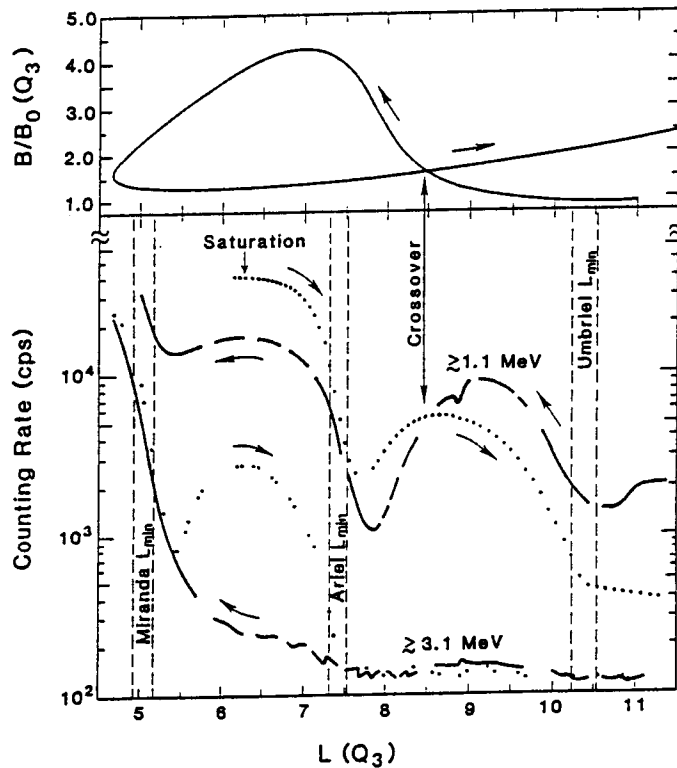

Figure 5

The ratios of the inbound and outbound counting rates at the same L value are inversely correlated to the ratios of the B/B_0 values. The inbound/outbound ratios for B/B_0 and the ≥ 1.1-MeV electron counting rates both pass through unity near $L \sim 8.5$. The inverse correlation effect arises from the increase in directional intensity for electrons at large pitch angles with respect to the vector directions of the local magnetic field. For pitch angle distributions of the form $j(\alpha) \sim \sin^{2n}\alpha$ (i.e., "pancake" distributions) the intensities would vary as $(B_0/B)^n$ for measurements with omnidirectional detectors. The inbound-outbound crossover at $L \sim 8.5$ therefore confirms the near omnidirectionality of the CRS detector (D1 in the Electron

Telescope) for ≥ 1.1-MeV electrons and also indicates that the trapped electron populations were stable at least over the six-hour time interval between the inbound and outbound measurements at that L-value.

The magnitude of the inbound-outbound ratios in Figure 5 can be used to estimate L-dependent values of the parameter n for pancake-type pitch angle distributions. A complication arises, however, since the counting rate profiles in Figure 1 do not include corrections for detector deadtime, which is especially significant at rates above 10^4 cps. Note that the ≥ 1.1-MeV rate reaches its saturation plateau level of $4-5 \times 10^4$ cps inbound at $L < 5$ and outbound at $L \leq 6.5$, where the incidence rate of MeV electrons is far higher than the observed rate. Thus the actual inbound-outbound intensity ratios are larger than indicated by the raw counting rates at levels $\geq 10^4$ cps. The deadtime effect is relatively insignificant for the ≥ 3.1-MeV electron profile between $L \sim 5$ and $L \sim 7$, where the counting rates are below 5×10^3 cps. The convergence of the inbound and outbound profiles near the minimum intensity point of the outbound Miranda signature indicates a nearly isotropic (i.e., $n \sim 0$) pitch angle distribution, given that the B/B_0 inbound/outbound ratio is 2.2. The intensity peak at $L \sim 6.5$ outbound corresponds to a much more anisotropic distribution with $n \sim 3$. The $\geq 1.1-$MeV profile in the vicinity of the Ariel signature also has a more anisotropic distribution with $n \geq 3$ for counting rates $\geq 10^4$ cps as compared to $n \sim 2$ at the signature minimum.

Displacement Effect for Satellite Sweeping Signatures. The locations in L of the intensity minima for most satellite sweeping signatures of MeV electrons lie outwards from the range of L_{min} values for each satellite. The only two exceptions are the inbound Miranda and outbound Umbriel signatures, which do not have recognizable local minima, probably due to relatively large local values of B/B_0 and associated effects of pitch angle distributions. Our most accurate measurements of the locations of the signature minima have been obtained from six-second counting rate data and are summarized in Table 1. Since the outbound Miranda signature is in the saturation region for $\geq 1.1-$MeV electrons, we have also used other integral counting rates with energy thresholds of $\geq 2.7-$MeV (6-s data) and $\geq 3.1-$MeV (96-s data) to calculate a mean L value of the local minimum for that signature. In some cases the larger uncertainties were also produced by data gaps. These data show that the signature minima lie at least 0.2 R_U ($R_U = 25,600$ km) outwards at the magnetic equator from the maximum L_{min} values. The largest displacements from the average L_{min} values are 0.4 R_U. The slightly different displacements in the inbound and outbound signatures for Ariel may be artifacts of the outbound data gap near the local minimum or of non-omnidirectional components in the response of the $\geq 1.1-$MeV detector.

The observed displacements may be important indicators of radial transport processes acting on trapped energetic particles in the magnetosphere of Uranus. In the absence of radial transport across field lines the minima of the satellite signatures would have been observed at the minimum-L positions where the satellite sweeping rates are maximal. Figure 6 illustrates the effect of diffusion as a function of time on a one-dimensional absorption signature in which trapped particles have a ramp-like initial absorption profile, being totally absorbed at $L = L_{min}$ ($X = 0$) and partially

absorbed with decreasing efficiency out to $L = L_{min} + b$ ($X = 1$), where b is the radial width of the signature. As time T increases for a constant diffusion coefficient D, the radial profile of the signature fills in most rapidly near the large density gradient at $L = L_{min}$, the effect at large times $T \gg 0$ being that the minimum density moves approximately to the mid-point of the initial absorption signature. The radial width parameter b for an actual satellite signature would need to be determined by more accurate calculations of sweeping rates as functions of a satellite's magnetic coordinates and by numerical modeling of diffusive transport to determine the width of the radial region at $L \gtrsim L_{min}$ in which satellite sweeping and diffusion are competitive processes. Although the sweeping process is inherently a time-dependent effect, due to the rapid changes in magnetic coordinates of the satellites, the observed signatures are most likely the result of a long-term balance between periodic episodes of satellite sweeping, the continuous effects of diffusion, and electron injection by external or internally distributed sources in the magnetosphere.
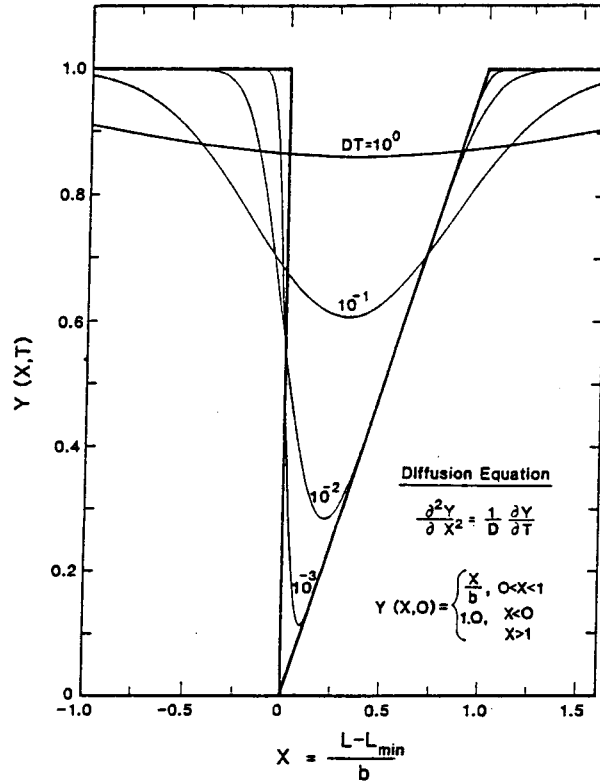

Figure 6

Laboratory Calibration for Magnetospheric Electrons. The CRS data from the Uranus encounter were largely dominated by the response of individual detector components to the large fluxes of energetic electrons at keV-MeV energies. Since accidental concidence rates induced by the large electron background virtually eliminated the possibility of multiple-coincidence analysis to determine electron energy distributions, the data analysis was confined mostly to the interpretation of counting rates and pulse height data from single, isolated detectors surrounded by various

amounts of shielding. Due to uncertainties about the electron response of some of these detectors we are using a beta-ray spectrometer in our laboratory to measure detector efficiencies for monoenergetic electrons at energies between 0.1 and 3.5 MeV. The use of a tiltable detector mount allows measurements over a wide range of beam incidence angles.

The main focus of this effort will be on the front D1 detector in the Electron Telescope (TET) which was pulse height analyzed in singles mode during the Uranus encounter. We will also test the response of a spare TET electronics system to high D1 counting rates to evaluate effects on D1 pulse height distributions and the calculation of differential energy spectra at 1-2 MeV from stopping electrons in D1. A secondary focus will be on the electron response of $450-\mu m$ silicon detectors in the four Low Energy Telescopes (LETs), which were used nominally for flux measurements of $\gtrsim$ 3-MeV protons but also showed relatively large responses to sub-MeV electrons in the Uranian magnetosphere. The beta spectrometer measurements have already been partially completed with the assistance of a Caltech undergraduate student during a summer undergraduate research (SURF) project. The remainder of the laboratory work will be completed during the fall of 1987.

Phase Space Density Analysis. The origin of the MeV electrons in the magnetosphere of Uranus is a question which may be resolvable by calculation of phase space densities from the energy spectra and radial profiles in the vicinity of the satellite absorption signatures. At constant values of the first and second magnetic invariants, M and K, an inwardly diffusing population of adiabatically accelerated electrons originating in the outer magnetosphere would always show a positive radial gradient in the phase space density, j/p^2, where j is the locally measured differential flux for electrons of momentum p. If an internal electron source were to make a significant contribution, such as might be provided by a magnetospheric recirculation process, the density gradient need not always be positive and local density minima would be found in satellite sweeping signatures. The special significance of the energetic electron signatures in the Uranian magnetosphere is that they are deep and broad enough to provide a substantive test of the inward diffusion theory.

The experimental resolution of this question depends critically on our evaluation of the D1 pulse height data from the TET. Our preliminary, post-encounter analysis found a general decline in phase space density towards closest approach in L to Uranus for electrons at energies above integral thresholds of 1-10 MeV, but cosmic ray background precluded measurements of integral energy spectra near the intensity minima of the satellite signatures. Further difficulties include the large corrections required to compute equatorial electron fluxes along portions of the spacecraft trajectory where B/B_0 changes rapidly. Note that the large inwards decline in the $\gtrsim$ 1.1-MeV counting rate (Figure 5) inbound from L $\sim$ 9 to the Ariel minimum at L $\sim$ 8 was largely due to the movement of Voyager 2 away from the magnetic equator. The local flux measurements in the inbound Umbriel signature were made, however, near the magnetic equator at $B/B_0 \leq 1.3$. Provisional results indicate a possible factor of two increase inwards in phase space density from the 1-2 MeV electron fluxes measured in this region. We are currently working to establish the statistical significance of this increase and will use the laboratory calibration results to evaluate potential instrumental effects.

Table 1

Positions of Minima in Satellite Signatures for MeV Electrons			
Satellite	L_{min}	L_{sig}	
		Inbound	Outbound
Miranda	4.9-5.2	5.38±0.04	5.38±0.08 [*,+]
Ariel	7.3-7.6	7.85±0.03	7.74±0.08 [+]
Umbriel	10.2-10.5	10.74±0.03	10.38±0.02 [**,+]

(*) Combined signatures for ≥ 1.1-,2.7-, and 3.1-MeV electrons.
(+) Larger uncertainty due to data gap.
(**) No local minimum, only an inflection point.

1.2.3. A Heavy Isotope Spectrometer Telescope (HIST) Launched on ISEE-3 in August 1978

HIST is designed to measure the isotope abundances and energy spectra of solar and galactic cosmic rays for all elements from lithium to nickel ($3 \leq Z \leq 28$) over an energy range from several MeV/nucleon to several hundred MeV/nucleon. Such measurements are of importance to the study of the isotopic constitution of solar matter and of cosmic ray sources, the study of nucleosynthesis, questions of solar-system origin, studies of acceleration processes and studies of the life history of cosmic rays in the galaxy.

HIST was successfully launched on ISEE-3 and provided high resolution measurements of solar and galactic cosmic ray isotopes until December 1978, when a component failure reduced its isotope resolution capability. Since that time, the instrument has been operating as an element spectrometer for solar flare and interplanetary particle studies.

Our work on solar flare, interplanetary, and galactic cosmic ray isotopes has resulted in the following recent talks and papers.

● "Solar Cycle Variations of Anomalous ^{4}He as Revealed by Studies of Cosmic Ray ^{3}He ," A. C. Cummings et al., *Bull. of Am. Phys. Soc.* **31**, 872 (1986).

● "^{3}He in Galactic Cosmic Rays," R. A. Mewaldt, *Ap. J.* **311**, 979 (1986).

● "A Re-Examination of the Cosmic Ray Helium Spectrum and the ^{3}He/^{4}He Ratio at High Energies ," W. R. Webber et al., *Ap.J.* **312**, 178 (1987).

● "Solar Cycle Variations of Anomalous ^{4}He as Deduced by Studies of Cosmic Ray ^{3}He," A. C. Cummings et al., *Geophys. Res. Letters.* **13**, 1043 (1986).

- "Solar Coronal Isotopic Abundances Derived From Solar Energetic Particle Measurements ," R. A. Mewaldt and E. C. Stone, *EOS Trans. AGU Nov.* **67**, 1142 (1986).

- "Isotopic Abundances of Solar Coronal Material Derived from Solar Energetic Particle Measurements," R. A. Mewaldt and E. C. Stone, *Bull. of the Amer. Astron. Soc.* **18**, 1042 (1986).

- "Solar Coronal Isotopic Abundances Derived from Solar Energetic Particle Measurements," R. A. Mewaldt and E. C. Stone, *Bull. of Amer. Phys. Soc.* **32**, 1037 (1987).

- "Galactic Cosmic Ray Isotope Spectroscopy: Status and Future Prospects," R. A. Mewaldt, *Proceedings of the 13th Texas Symposium on Relativistic Astrophysics*, p. 573, World Scientific (1987).

- "Isotope Abundances of Solar Coronal Material Derived from Solar Energetic Particle Measurements ," R. A. Mewaldt and E. C. Stone, *Proceedings of the 20th International Cosmic Ray Conference, Moscow, USSR* **3**, 255 (1987).

A summary of one of these appears below.

Isotope Abundances of Solar Coronal Material
Derived from Solar Energetic Particle Measurements

Although the Sun contains more than 99% of solar system material, most of our present knowledge of the solar system element and isotope distribution comes from studies of terrestrial, meteoritic, and lunar material. Spectroscopic studies of the solar composition are subject to a number of sources of uncertainty, and in the case of isotopic abundances, are available for only a few elements. Measurements of solar energetic particles (SEPs) accelerated during large solar flares provide a means of sampling directly the composition of solar material, and thereby determining its composition. However, in interpreting such measurements, there has always been a question of the extent to which the observed particle composition might have been fractionated, during either the acceleration process, or the subsequent propagation through interplanetary space.

Recently, a Voyager study by Breneman and Stone (hereinafter B&S) provided an answer to this question. By combining elemental composition measurements from 10 large flares with ionic charge-state measurements, B&S showed that the ionic charge-to-mass ratio (Q/M) is the principal organizing factor for the fractionation of SEP elemental abundances by acceleration and propagation processes, and for flare-to-flare composition variations. They found that these variations are a smooth function of Q/M that is well described by a power law. By correcting for these fractionation effects, B&S derived unfractionated coronal abundances for 20 elements. An extension of the B&S approach has been applied to SEP isotope measurements.

Most of the measurements used for this study were obtained by the Caltech Heavy Isotope Spectrometer (HIST) on ISEE-3 during the large solar flare of 9/23/78. When these measurements were originally published the relative isotope abundances were reported essentially as observed, with no corrections for any possible fractionation. To determine the magnitude and Q/M-dependence of the fractionation in the 9/23/78 flare event we make use of the charge-state measurements made during this flare on the same spacecraft by the Max-Planck/Maryland group, and of the elemental composition measured by our own experiment. Figure 7 plots the ratio of the abundances measured in this event to the B&S SEP-derived coronal abundances as a function of Q/M. Note that in this flare elements that retain several electrons, such as Fe, Si, and S, are depleted relative to those elements that are nearly fully stripped, such as C. As in the B&S study, this fractionation is well described by the function $(Q/M)^\alpha$, where a least squares fit gives $\alpha = 1.95 \pm 0.44$. From this dependence we would also expect heavy isotopes such as ^{22}Ne to be slightly depleted in this flare relative to lighter elements such as ^{20}Ne.
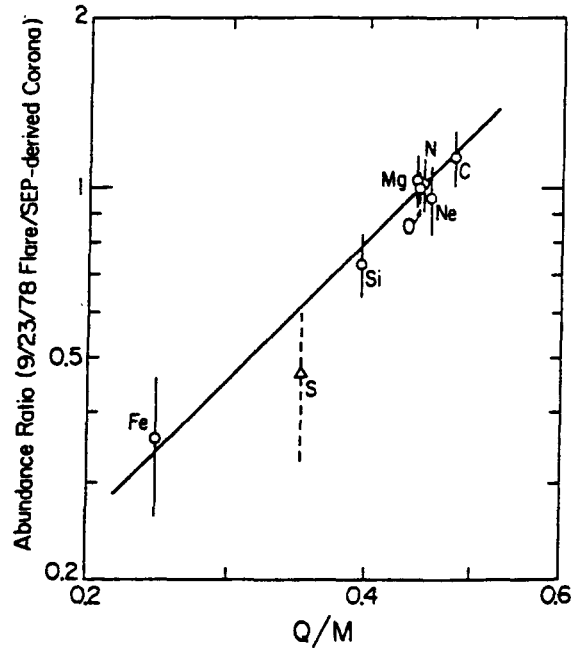

Figure 7

To correct for the effects of fractionation in this flare and thereby obtain measurements of the coronal isotopic composition we use

$$\frac{S_i}{S_j} = \left[\frac{M_i}{M_j} \right]^\alpha \left[\frac{N_i}{N_j} \right] \qquad (1)$$

where S_i and S_j are the coronal abundances of isotopes i and j of a given element with masses M_i, M_j, where N_i and N_j are the observed abundances, reported previously, and where $\alpha = 1.95$.

We have also considered the magnitude of fractionation effects on solar flare isotope results reported by others. To do this we note from Fig. 8 that a reasonable estimate of the value of α for a particular flare can be obtained simply from $(Fe/O)_f$, the Fe to O ratio of the flare measured in the same experiment. We then use:

$$\alpha_{est} = \frac{\ln[(Fe/O)_f/(Fe/O)_c]}{\ln[(Q/M)_{Fe}/(Q/M)_O]} \qquad (2)$$

where $(Fe/O)_c$ is the coronal Fe to O ratio from B&S. As an estimate of the charge states of Fe and O we use the average values $Q(Fe) = 14.9 \pm 0.09$ and $Q(O) = 7.00 \pm .02$ from Luhn et al., noting that in large flares the charge states do not appear to vary significantly from flare to flare. We then use Eqn. 1 to obtain an estimate of the coronal abundance.
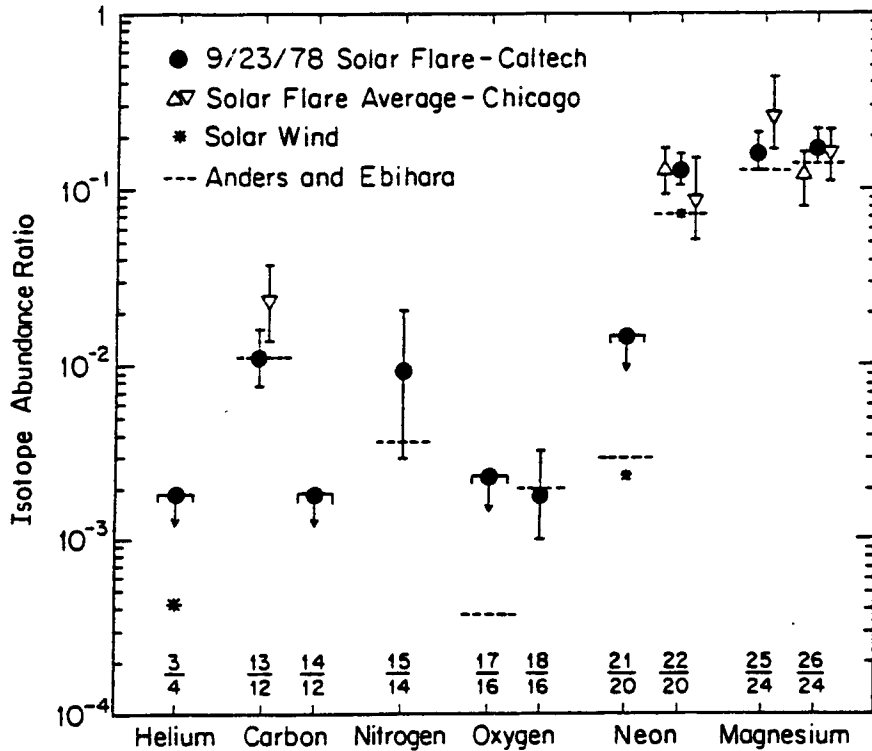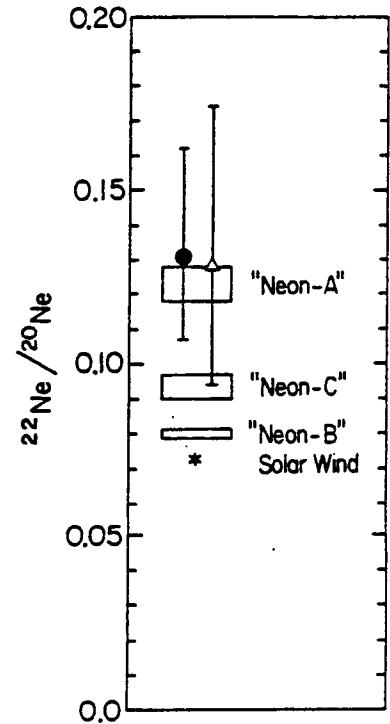

Figure 8

Figure 9

In Figure 8 we compare our derived coronal composition measurements with the "solar system" abundances of Anders and Ebihara and with the solar wind measurements of Geiss et al. Also shown in Fig. 8 are various flare-average measurements reported by the Chicago group, corrected for fractionation effects as described above. Note in Fig. 8 that the $^{13}C/^{12}C$, $^{15}N/^{14}N$, $^{18}O/^{16}O$, $^{25}Mg/^{24}Mg$, and $^{26}Mg/^{24}Mg$ ratios that we obtain for the corona are consistent with the Anders and Ebihara compilation, in agreement with our earlier conclusions based on the measured

ratios, uncorrected for fractionation effects. This is not surprising because the magnitude of the fractionation correction is not large (typically 10-20%).

The isotope ^{22}Ne is of special interest because of the wide range of ^{22}Ne/^{20}Ne ratios observed in various samples of solar system material. The isotopic composition of neon in the Sun is controversial, with Anders and Ebihara adopting the solar wind (SW) value as a standard, while Cameron adopts the meteoritic component neon-A for solar system neon. Figure 9 shows selected solar system ^{22}Ne/^{20}Ne measurements on an expanded scale, including neon-B (directly implanted solar wind). As noted before, the spacecraft measurements of ^{22}Ne/^{20}Ne in SEPs are inconsistent with the SW ^{22}Ne/^{20}Ne ratio. Note that the result of correcting our SEP measurements for fractionation effects has increased the magnitude of this difference rather than narrowing it.

Figure 9 also includes the component neon-C observed in lunar material, which has been interpreted to represent implanted SEP neon. Recent measurements by the Swiss group confirm that there is a difference between neon-C and the measured solar wind ^{22}Ne/^{20}Ne ratio. It should be pointed out that there should presumably also be a fractionation correction applied to the neon-C measurements. While the magnitude of this correction is difficult to estimate, it is probably not large, and the average Fe/O ratio measured in large solar flares at a similar energy (~ 1 MeV/nucleon) suggests that the measured neon-C ratio should be multiplied by a correction factor of ~ 1.1.

In our first report of SEP ^{22}Ne/^{20}Ne ratios we suggested that the difference between the measured SEP and SW isotope ratios could result from fractionation of either the SEP or SW abundances, both of which are presumably derived from coronal material. We have now measured and corrected for the fractionation in SEPs and find that the resulting value for ^{22}Ne/^{20}Ne in the corona differs from the measured SW value to an even greater extent, while we obtain quite reasonable values for the coronal isotopic composition of the other elements studied. Isotope fractionation during solar wind acceleration remains as a possibility for explaining this difference.

1.2.4. A Heavy Nuclei Experiment (HNE) Launched on HEAO-C in September 1979

The Heavy Nuclei Experiment is a joint experiment involving this group and M. H. Israel, J. Klarmann, W. R. Binns (Washington University) and C. J. Waddington (University of Minnesota). HNE is designed to measure the elemental abundances of relativistic high-Z cosmic ray nuclei ($17 \leq Z \leq 130$). The results of such measurements are of significance to the studies of nucleosynthesis and stellar structures, the existence of extreme transuranic nuclei, the origin of cosmic rays, and the physical properties of the interstellar medium. HNE was successfully launched on HEAO-3 and operated until late May 1981.

The following talks and paper were presented during the reporting period:

● "Measurements of Ultraheavy Cosmic Rays with HEAO-3," W. R. Binns et al., *for publication in Essays in Sp. Sci.* (submitted 1985).

● "Fragmentation Cross Sections of Ultraheavy Nuclei," M. P. Kertzman et al., *Bull. of Am. Phys. Soc.* **31**, 871 (1986).

● "Elemental Abundances of Ultraheavy Cosmic Rays Measured on HEAO-3," B. J. Newport et al., *Bull. of Am. Phys. Soc.* **31**, 871 (1986).

● "The Abundances of Ultraheavy Elements in the Cosmic Radiation," B. Newport, Ph.D. Thesis, California Institute of Technology (1986).

● "Cosmic-Ray Energy Spectra Between Ten and Several Hundred GeV/amu for Elements from $_{18}$Ar to $_{28}$Ni--Results from HEAO-3," M. H. Israel et al., *Proceedings of the 20th International Cosmic Ray Conference, Moscow, USSR* **1**, 330 (1987).

● "Anisotropy of Galactic Iron of Energy 30 to 500 GeV/amu Studied by HEAO-3," T. L. Garrard et al., *Proceedings of the 20th International Cosmic Ray Conference, Moscow, USSR* **1**, 348 (1987).

● "The Abundances of Ultraheavy Elements in the Cosmic Radiation," E. C. Stone et al., *Proceedings of the 20th International Cosmic Ray Conference, Moscow, USSR* **1**, 366 (1987).

● "Release of Nuclei from Relativistic Nucleus-Nucleus Interactions," C. J. Waddington et al., *Proceedings of the 20th International Cosmic Ray Conference, Moscow, USSR* **2**, 152 (1987).

● "The Energy Dependence of Fragmentation Cross-Sections of Relativistic Heavy Nuclei," C. J. Waddington et al., *Proceedings of the 20th International Cosmic Ray Conference, Moscow, USSR* **2**, 149 (1987).

● "Response of Ionization Chambers and Cerenkov Counters to Relativistic Ultraheavy Nuclei," J. Klarmann et al., *Proceedings of the 20th International Cosmic Ray Conference, Moscow, USSR* **2**, 390 (1987).

Deviations from Z^2 Scaling

In our 1986 run at the Lawrence Berkeley Laboratory, in addition to the cross-section measurements which were the primary goal of the calibration, we also measured deviations from Z^2 scaling in ionization and energy loss. Both resolution and stability were improved compared to our 1984 run. A schematic illustration of the calibration instrument is shown in Figure 10. The instrument consisted of a stack of ionization chambers and a Cerenkov detector.

beam

I.C.-1

target
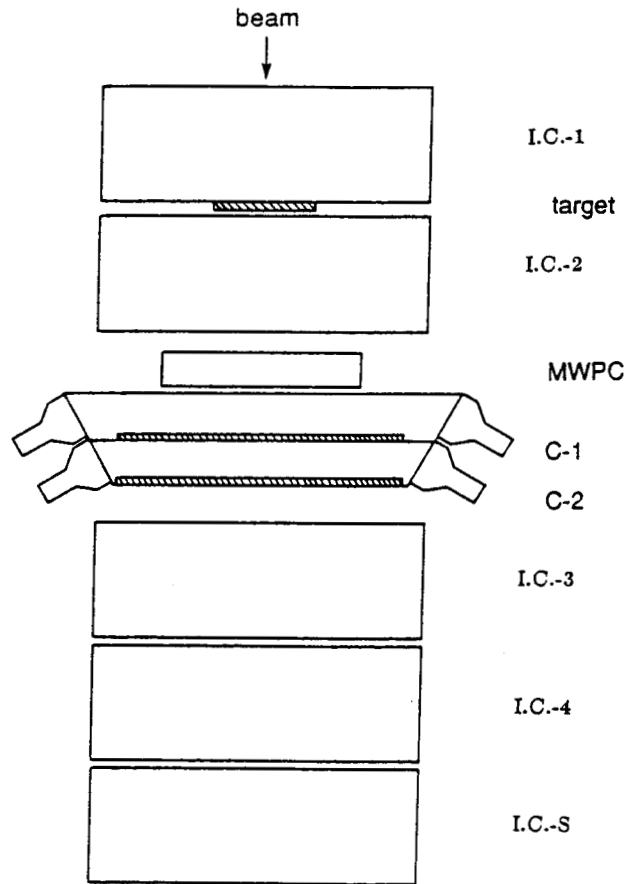
I.C.-2

MWPC

C-1

C-2

I.C.-3

I.C.-4

I.C.-S

Figure 10

In Figure 11 we show the ratio of the measured ionization signal in the front chamber (I.C.-1) to the tabulated energy loss calculations of Barkas and Berger as a function of energy in the detector. The energy is measured at the top of the stack using the LBL beam 40 bending magnet; within the stack the energy in any particular detector is determined using the Barkas and Berger range function. For this figure, the energy in the detector is very near the beam energy. The ratio is arbitrarily normalized, with the same normalization factor used for all following data plots. The data show small negative deviations from Z^2 and relatively large deviations from the predicted energy dependence (as we reported earlier based on the 1984 runs).

We showed, in our Moscow ICRC talk, that the deviations from the predicted Barkas and Berger energy dependence can be understood as an effect of the loss of knock-on electrons from the back side of the ionization chamber, with no compensation from knock-ons in preceding material. If we look at the chambers which have preceding material, such as ion chamber 3 (see Figure 12) or 4 behind the Cerenkov detector or ion chamber 2 when a thick target is present, then the energy dependence is much closer to that predicted from the Barkas and Berger tables.
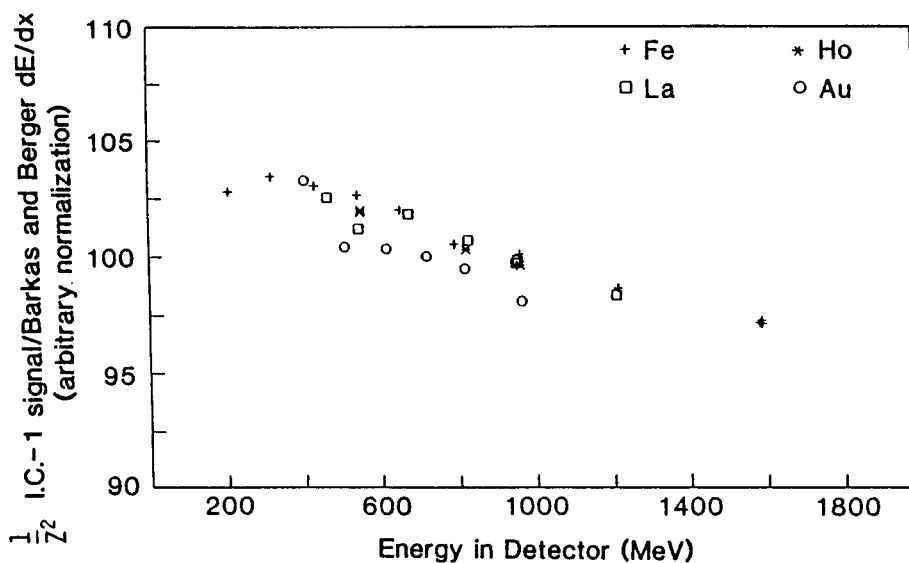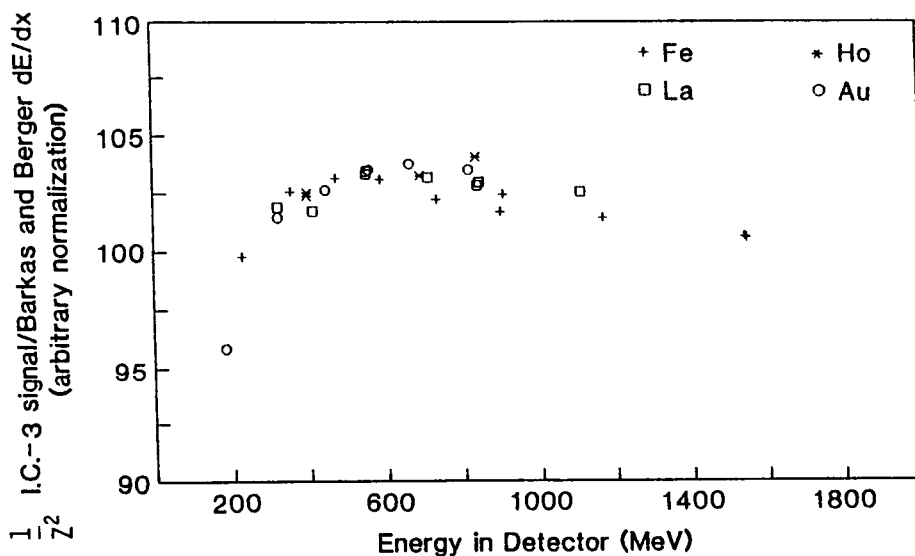
Figure 11

Figure 12

In all these cases the deviations from Z^2 are quite small, smaller than would be predicted based on the work of Ahlen, Salomon, and co-authors for instance. We are working to explain this as an effect of knock-on transport also, but have only limited qualitative success at this point. Quantitative understanding of these deviations from Z^2 scaling will require additional study of all the terms listed by Ahlen -- Mott scattering, Bloch and relativistic Bloch corrections, charge pickup, et cetera. Some of the necessary data should come from other LBL measurements soon. In any case, our primary goal of demonstating that our interpretation of the HEAO HNE flight data is reasonable has been achieved. These detectors are well suited for cosmic-ray charge measurement.

1.2.5. Proposal for an Advanced Composition Explorer (ACE)

This investigation, submitted to NASA for the Explorer Concept Study Program, was proposed jointly by this group, and by R. E. Gold and S. M. Krimigis (APL/JHU), G. Geiss (University of Bern), J. A. Simpson and M. E. Wiedenbeck (University of Chicago), L. F. Burlaga and T. T. von Rosenvinge (GSFC), W. C. Feldman (LANL), G. Gloeckler and G. M. Mason (UMd) and D. Hovestadt (MPI). This Explorer-class mission would make comprehensive measurements of the elemental and isotopic composition of accelerated nuclei with increased sensitivity of several orders of magnitude, and with improved mass and charge resolution. ACE would observe particles of solar, interplanetary, and galactic origins, spanning the energy range from that of the solar wind ($\sim$ 1 keV/nucleon) to galactic cosmic ray energies (several hundred MeV/nucleon). Definitive studies would be made of the abundance of essentially all isotopes from H to Zn ($1 \leq Z \leq 30$), with exploratory isotope studies extending to Zr ($Z=40$), and element studies extending to U ($Z=92$).

ACE would be a coordinated experimental and theoretical effort, designed to investigate a wide range of fundamental problems. In particular, ACE would provide the first extensive tabulation of solar *isotopic* abundances based on direct sampling of solar material and would establish the pattern of *isotopic differences* between galactic cosmic ray and solar system matter. These composition data would be used to investigate basic dynamical processes that include the formation of the solar corona, the acceleration of the solar wind, and the acceleration and propagation of energetic nuclei on the Sun, in interplanetary space, and in cosmic ray sources. They would also be used to study the history of solar system material and of galactic cosmic ray material, and to investigate the differences in their origin and evolution.

The ACE study payload includes five high resolution spectrometers, each designed to provide the ultimate charge and mass resolution in its particular energy range, and each having a collecting power 1 to 3 orders of magnitude greater than previous or planned experiments. Included in the study would be two spectrometers, a Solar Isotope Spectrometer (SIS) and a Cosmic Ray Isotope Spectrometer (CRIS), for which Caltech would play a leading role. These spectrometers would make use of the proven mass-resolution techniques and large-area detectors that were developed and tested by this laboratory over the past decade, partly through the support of this grant.

1.2.6. Galileo Heavy Ion Counter

This experiment, constructed by this group in collaboration with N. Gehrels at Goddard Space Flight Center, has been added to the Galileo mission as an engineering subsystem. It will monitor penetrating ($\sim$ 10 to $\sim$ 200 MeV/nucleon) sulfur, oxygen, and other heavy elements in the Jovian magnetosphere with the sensitivity needed to warn of potential "single-event upsets" (SEU) in the attitude control system computer. (SEUs are state changes induced by ionizing radiation.) Caltech is responsible for management, detector testing, and calibration of the experiment, which is based on repackaging the Voyager CRS prototype unit (the PTM). Although the primary

purpose is engineering support, the data will allow us to continue our investigation of spectra of trapped ions in the Jovian magnetosphere and their relation to the Jovian aurora. In addition, during cruise phase and in the outer Jovian magnetosphere, we will use the instrument to measure the elemental composition of solar flare events and of the anomalous cosmic ray component.

Current activities include response to new constraints due to mission redesign and attempting to maintain instrument reliability in the face of greatly extended ground handling.

1.2.7. Models of Saturn's Magnetic Field

The analysis of the models of Saturn's magnetic field in the region between 1 and 8 Saturn radii using Pioneer 11, Voyager 1, and Voyager 2 data now shows that the part of the field due to internal sources shows no significant change over the period of the three encounters and no observable deviations from axial symmetry. The apparent deviations of the Z_3 model of Connerney, Ness, and Acuña from this model are due in part to their use of 60,000 km as the unit for r, the distance from the center of Saturn, in their first paper and their use of 60,330 km in all later papers without making the appropriate changes in the values of g_1^0, g_2^0, and g_3^0. The g_3^0 value of the Z_3 model differs from that of the $P_{11}84$ model and from any model based on the data of all three encounters by about 20%. Whichever value of g_3^0 is used for the fit to the Voyager data, the closeness of fit of the model to data is not significantly changed. But the closeness of fit to the P_{11} data, or to the data of all three spacecraft, is much better for the $P_{11}84$ model or the model based on all three data sets. The reason for this is that the contribution of the g_3^0 coefficient to the modeled field varies as $1/r^5$ and varying this coefficient makes very little change in the model's predictions along the Voyager trajectories. The minimum r on the P_{11} trajectory is half that for the Voyagers and the accuracy with which g_3^0 can be determined is 30 times that for Voyager 2 and 50 times that for Voyager 1. A preliminary estimate of the internal source coefficients based on all three data sets is $g_1^0 = .2115$, $g_2^0 = .0156$, $g_3^0 = .0230$.

The electrical current systems in the region outside the surface of Saturn makes a contribution of the order of 10 nT to the magnetic field in the shell between 1 and 10 R_s where our model is to be used. This contribution varies substantially from one encounter to another and from the inbound to the outbound side of Saturn. If the currents were all outside 8 R_s and were constant during each encounter, the field generated inside 8 R_s could be described by the external source coefficients G_n^m, H_n^m, whose values might change between encounters. As Connerney, Acuña and Ness (Nature 292, 726-742, 1981) pointed out, there must be current in the region inside 8 R_s whose magnetic field can not be accurately modeled by spherical harmonic coefficients. They assumed that the ring current was axially symmetric but added small G_1^1 and H_1^1 coefficients to model the fields due to small non-axisymmetric current systems outside 8 R_s. In our subsequent analyses we find that the ring current is not axially symmetric and that it varies substantially from one encounter to the next and perhaps during an encounter. It seems impossible with the limited data available to

determine with any precision these current distributions and the magnetic fields they produce. The Z_3 model provided a reasonable approximation to the field produced by these external current systems by determining the G_1^0, G_1^1, and H_1^1 coefficients that give the best fit of the Z_3 model to the data. We improve significantly the fit of our model to the observed data by using different values of these external source coefficients for each of the three encounters and using different values of G_1^0 on the inbound and outbound parts of each encounter. G_1^0 was always substantial smaller on the down-wind side of Saturn than on the up-wind side. This demonstrates that the ring current that makes this contribution to the magnetic field is not axially symmetric. The current density must be smaller and must extend further down the tail than on the sunward side.

2. Gamma Rays

This research program, which has received significant support from Caltech, is directed toward the investigation of galactic, extragalactic, and solar gamma rays with spectrometers of high angular resolution and moderate energy resolution carried on spacecraft and balloons. The main efforts have been directed toward the following two categories of experiments.

2.1. Activities in Support of or in Preparation for Spacecraft Experiments

These activities generally embrace prototypes of experiments on existing or future NASA spacecraft and they complement and/or support such experiments.

2.1.1. Gamma-Ray Imaging Payload (GRIP)

The GRIP instrument had two successful flights during the period covered by this status report. In October, 1986, the instrument was launched on its maiden flight from Palestine, Texas. During the 28 hour flight, the instrument imaged several fields-of-view with 0.6° resolution including the Crab, Cygnus, and Galactic Center regions. Preliminary data analysis has yielded images of the Crab and Cygnus regions in which the Crab nebula and Cyg-X1 are clearly detected. The Crab pulsar has also been detected using the characteristic pulse signature. The first flight verified the performance of the instrument in several important areas. First, the pointing system was verified to be stable to a level of approximately 0.1° sigma with ex post facto correction to better than 0.1° relative accuracy. The point spread function of the Crab and Cygnus images agreed with the expected 0.6° resolution of the instrument. Second, the measured energy resolution in flight was as good as that on the ground, being 5% FWHM at 2.22 MeV. Third, the in-flight background was approximately as anticipated, being dominated by aperture flux at low energies and shield leakage at high energies.

Detailed analysis of the data from the first flight was in progress when SN1987a occurred on February 23, 1987. Concentration was immediately focussed on preparation for a possible flight from the Southern Hemisphere for observations of the supernova. After submission of a supplementary proposal for Southern Hemisphere observations and acceptance by NASA, an expedition to Alice Springs, NT was planned and carried out. The GRIP instrument was assembled briefly at Caltech, then disassembled and shipped to Alice Springs, where it was reassembled and prepared for flight. The instrument was launched on May 19 (U.T.) for an 11 hour flight, including approximately 8 hours of observations at float. The observation time was dedicated primarily to SN1987a, three 1/2 hour periods being used for calibration observations on the Crab nebula.

The experience gained from the preliminary analysis of the first flight aided significantly in a quick turnaround of the data from the supernova observations. In addition to the PDP 11/24 GSE, a MicroVAX computer was also shipped to Alice Springs and an Ethernet connection established to provide a suitable environment for quick analysis. Images of the Crab were obtained using telemetry data within three days after the flight. After recovery and return of the on-board recorded flight tapes, pointing corrections were applied to the Crab data yielding images co-aligned to within 0.1° for the three separate 1/2 hour periods. This indicated that the supernova data could be added with confidence for the period of prime observations of the supernova. The resulting images of the LMC region, produced within 7 days of the flight, yielded no evidence of continuum or line flux from the supernova. Upper limits were calculated for the 847, 1238, and 2598 keV lines of ^{56}Co and subsequently announced in an IAU Circular. Work is currently in progress on determination of continuum upper limits in the range 30 keV to 9 MeV.

A third flight of the instrument is planned from Australia in October or November, 1987. Unfortunately, the instrument suffered a rather hard landing after the May flight. Although the primary telescope was not harmed, damage did occur to the platform structure and several instrument subsystems. The affected parts were shipped back to the U.S., while the bulk of the instrument was stored in Alice Springs. A detailed assessment of refurbishment requirements is in progress.

A preliminary report on this work to be presented at the International Cosmic Ray Conference in Moscow follows:

First Flight of a New Balloon-Borne Gamma-Ray Imaging Telescope

The GRIP instrument is a balloon-borne imaging γ-ray telescope for galactic and extra-galactic astronomy observations. The telescope employs a rotating lead coded-aperture mask and a large-area shielded NaI(Tl) scintillation camera to achieve good flux sensitivity over the energy range from 30 keV to 5 MeV and an imaging capability of 1070 0.6 degree pixels over a 20 degree field of view.

A schematic view of the GRIP detector system is shown in Figure 13. The primary detector is a position-sensitive NaI(Tl) scintillator viewed by 19 photomultiplier tubes (PMTs) which are individually pulse-height analyzed.

Background in the primary detector is reduced by an active anti-coincidence shield. The side of the shield consists of 12 plastic scintillator modules which form a cylinder ~16 cm thick. Each module is viewed by a single 5" PMT. The lower shield section is identical to the primary camera plate.
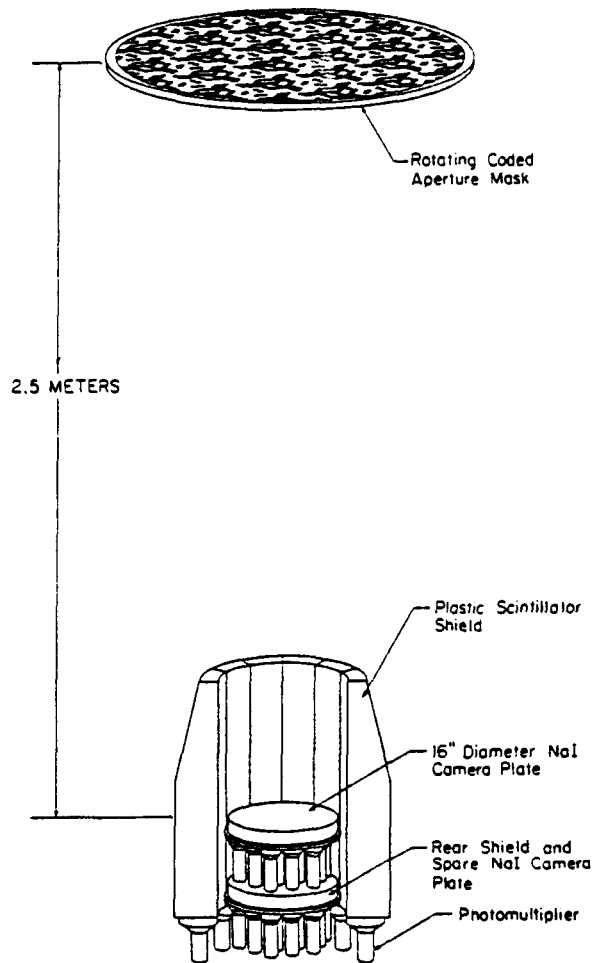

Figure 13

The coded aperture is located 2.5 meters from the detector and is composed of 2000 cells of which half are open and half contain a lead hexagon 2 cm thick and 2.5 cm flat to flat. The pattern of open and filled cells forms a hexagonal uniformly redundant array that is optimal for coded aperture imaging .

During an observation the mask is continuously rotated to impose a time modulation of the γ-ray signal at each location on the detector. Due to the antisymmetry of the coded-aperture pattern under 60 degree rotation (open and closed cell interchange for all but the central cell) the γ-ray signal at each detector position is modulated with a 50% duty cycle. This feature allows a complete background subtraction to be performed for each position on the detector, once every 20 seconds. In addition, the continuous rotation permits extension of the field of view to 20 degrees, increasing the number of pixels imaged by about a factor of ten.

The telescope is mounted on an elevation/azimuth pointing platform which utilizes active magnetometer feedback. Two magnetometers provide aspect information permitting post-flight correction for pointing inaccuracies. The telescope pointing system is under microprocessor control, allowing steering by ground command or the execution of a pre-programmed flight plan.

Gamma-ray event data and engineering data are recorded on-board and can also be telemetered to the ground for real-time analysis and redundant recording. The on-board data recording system was developed for high capacity (25 Gbyte) and bandwidth (1.4 Mbit/s) using commercial VCRs and audio digitizers.

GRIP was launched for its first flight at 14:18:25 UT October 15, 1986 from Palestine, Texas and landed 28 hours later in the southeast corner of Arkansas. The functionality of the instrument was verified in real time via imaging of both an on-board calibration source and the black hole candidate Cygnus X-1. Detailed analysis of the instrument's in-flight performance is now in progress. However, the major subsystems, including the detector and shield, the rotating lead mask, and the pointing system, have already been shown to have performed as expected.

The in-flight background spectrum measured by the NaI detector is shown in Figure 14. The line feature at 2.22 MeV is due to neutron capture on protons in the plastic shield. The line at 1.46 MeV is probably due to ^{40}K in instrument material and has nearly the same intensity as on the ground. The line feature near 0.5 MeV is likely a blend of lines at 472 and 511 keV due to inelastic neutron scattering on Na and positron annihilation.
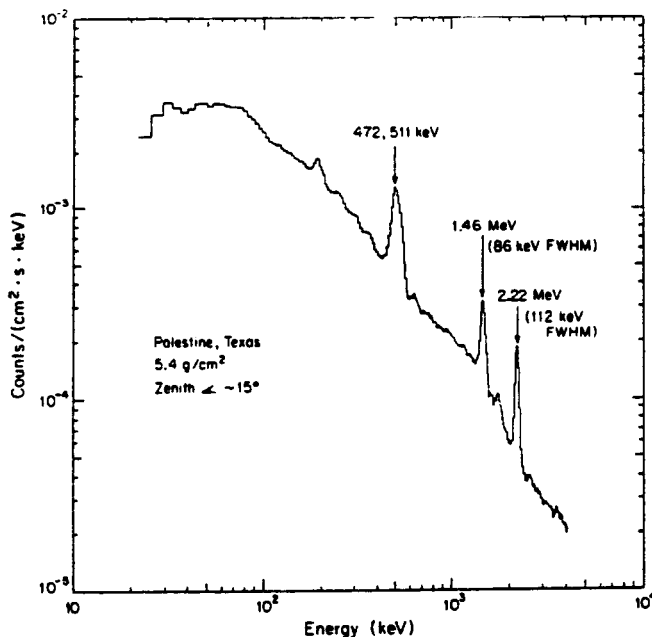

Figure 14

The 5% FWHM energy resolution measured for the in-flight 2.22 MeV background line is consistent with resolution performance obtained on the ground, as can be seen by comparison to Figure 15, an energy spectrum measured in the laboratory using a ^{228}Th source. The good in-flight energy resolution of the detector, which approaches that of the best single PMT NaI(Tl) detectors, is the result of detailed mapping of the detector response as a function of event location and the successful operation of an array of light emitting diodes for continuous in-flight PMT gain monitoring.
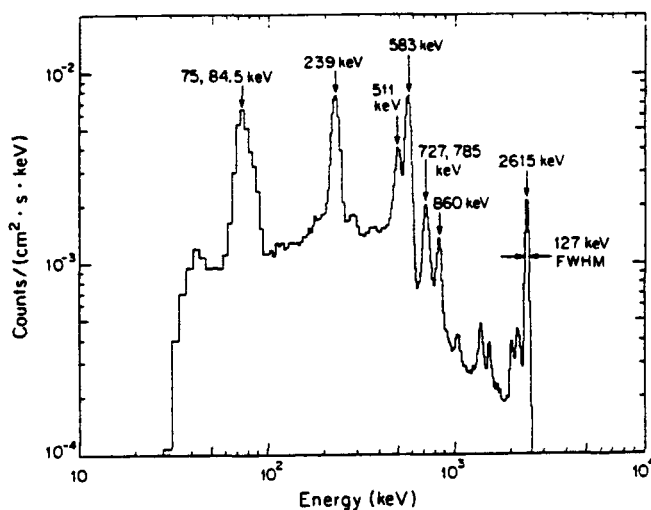
Figure 15

Much of the observing time for the first flight was devoted to the Crab and Cygnus regions which contain the two most intense gamma-ray sources in our energy range: the Crab Nebula and Cygnus X-1. These objects can be imaged in less than 15-minutes and can therefore be examined for variability on these time scales. Such studies are currently in progress as is the determination of the overall spectral characteristics of these sources. The objects also provide important functional checks on the performance of the pointing system over a wide range of azimuth and elevation.

Figures 16 and 17 show preliminary images of the Crab and Cygnus regions based on two-hour exposures over the energy range 50 to 150 keV. Each figure shows a 20-degree diameter field of view with dashed lines indicating right ascension and declination coordinates. The positions of candidate sources are marked by crosses. The Crab Nebula and Cygnus X-1 are clearly identified at the 13 and 19 sigma levels respectively. The finite widths of the image peaks for the Crab Nebula and Cygnus X-1 are due to the instrumental resolution of approximately 0.6 degrees, and the measured source locations are consistent with the current estimated pointing uncertainty.
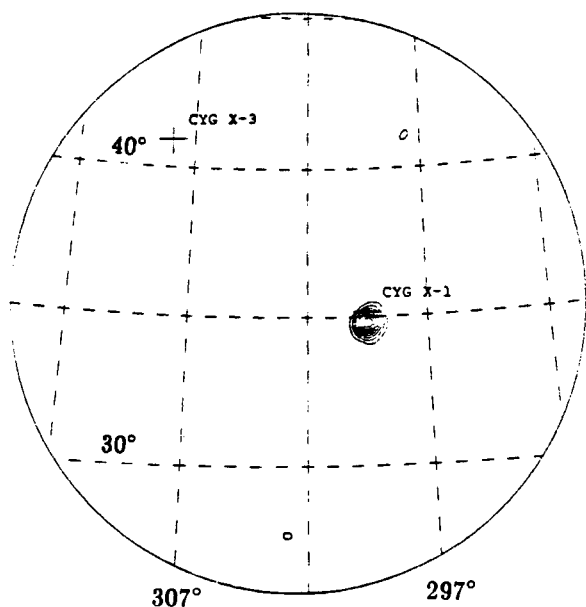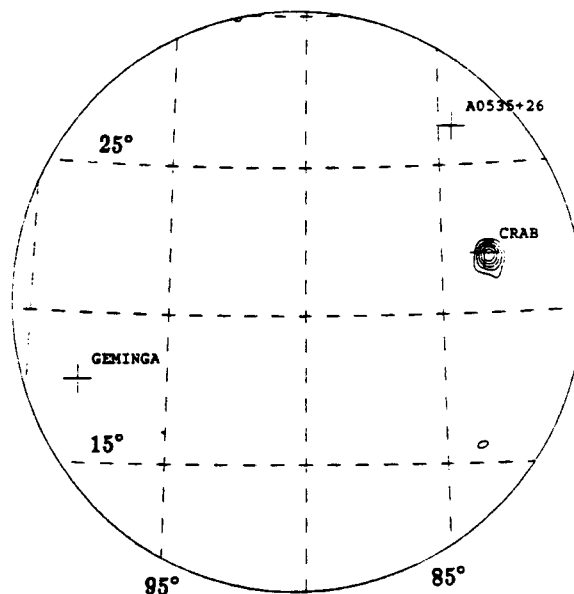
Figure 16   Figure 17

In addition to the Crab Nebula and Cygnus X-1 there are several features in Figures 16 and 17 which appear above the 3-sigma level. However, these are likely due to statistical fluctuations which are expected to produce on average 6 such features in each image. The candidate sources Cygnus X-3, Geminga, and A0535+26 are not seen in these images. However, specification of flux limits or possible detection of these sources awaits work in progress to verify instrument sensitivity and the processing of the full 6-hour exposure for each source region.

2.1.2. Development of γ-Ray Imagers with Very High Angular Resolution

We have continued work on the definition and design of ultra-high resolution γ-ray imagers for solar and cosmic γ-ray astronomy. Above 100 keV, past instruments have been limited to a typical angular resolution of 10° or poorer. Extensions of current technology will allow γ-ray imaging with angular resolution approaching one second of arc. Most of the work in this area has been supported under other NASA grants and contracts.

During the summer of 1986, two proposals were submitted to the Explorer concept study program. The first was a proposal for the study of an arc-second gamma-ray imager for solar observations (GRID) undertaken with collaborators from NASA Goddard Space Flight Center, Southampton Univ., Mullard Space Science Laboratories, Los Alamos Scientific Laboratories, Univ. of California at San Diego, Univ. of Birmingham, Yale, NASA Marshall Space Flight Center, Delft Univ., and the Naval Research Laboratory. The second proposal was submitted in collaboration with University of California at Berkeley to study the design of a high-angular resolution

all-sky imaging instrument (HEASI). The team involved in the GRID proposal has worked during the last year to develop plans for an advanced high-resolution imager for long-duration balloon observations during the next solar maximum. We have been working in particular with investigators at GSFC, MSFC, Delft, and UCSD on this project, which is now entering a detailed definition stage.

3. Other Activities

R. A. Mewaldt is serving as a member of NASA's High Energy Astrophysics Management Operations Working Group (HEAMOWG) and the Cosmic Ray Program Working Group (CRPWG). He is also a member of the Superconducting Magnet Facility (Astromag) Definition Study Team, where he is chairman of the Science and Facility Subcommittee.

T. A. Prince has received a Presidential Young Investigator Award from the National Science Foundation and is serving as a member of the Gamma-Ray Astronomy Program Working Group (GRAPWOG), the Max '91 Science Study Committee, and the Pinhole/Occulter Facility Science Working Group.

E. C. Stone continues to serve as NASA's Project Scientist for the Voyager Mission. He is also a member of the Commission on Physical Sciences, Mathematics, and Resources of the National Research Council.

4. Bibliography

Althouse, W. E., W. R. Cook, A. C. Cummings, M. H. Finger, D. M. Palmer, T. A. Prince, S. M. Schindler, C. H. Starr, and E. C. Stone, "First Flight of a New Balloon-Borne Gamma-Ray Imaging Telescope," *Proceedings of the 20th International Cosmic Ray Conference, Moscow, USSR* 1, 84 (1987).

Christian, E. R., J. E. Grove, R. A. Mewaldt, S. M. Schindler, T. Zukowski, J. C. Kish, and W. R. Webber, "High Resolution Cerenkov Detectors for Use in a Cosmic Ray Isotope Spectrometer ," *Proceedings of the 20th International Cosmic Ray Conference, Moscow, USSR* 2, 382 (1987).

Christian, E. R., J. E. Grove, R. A. Mewaldt, S. M. Schindler, and E. C. Stone, "Cosmic Ray Isotope Measurements with a High Energy Spectrometer," *Proceedings of 20th International Cosmic Ray Conference, Moscow, USSR* 1, 364 (1987).

Christon, S. P., E. C. Stone, and J. T. Hoeksema, "Evidence for a Latitudinal Gradient of the Cosmic Ray Intensity Associated with a Change in the Tilt of the Heliospheric Current Sheet," *Geophys. Res. Letters.* 13, 777 (1986).

Cooper, J. F., E. C. Stone, and W. E. Webber, "Satellite Signatures from MeV Electrons in the Magnetosphere of Uranus," *EOS Trans. AGU Nov.* 67, 1174 (1986).

Cooper, J. F., A. E. Metzger, and E. L. Chupp, "Mercury 2000: Stereoscopic Observations of Gamma Ray Flares," *Proceedings of the 20th International Cosmic Ray Conference, Moscow, USSR* 4, 395 (1987).

Cummings, A. C., R. A. Mewaldt, and E. C. Stone, "Solar Cycle Variations of Anomalous ^{4}He as Revealed by Studies of Cosmic Ray ^{3}He ," *Bull. of Am. Phys. Soc.* 31, 872 (1986).

Cummings, A. C., E. C. Stone, and W. R. Webber, "Observation of a Large Negative Latitudinal Gradient of Anomalous Oxygen," *EOS Trans. AGU Nov.* 67, 1150 (1986).

Cummings, A. C., R. A. Mewaldt, and E. C. Stone, "Solar Cycle Variations of Anomalous ^{4}He as Deduced by Studies of Cosmic Ray ^{3}He," *Geophys. Res. Letters.* 13, 1043 (1986).

Cummings, A. C. and E. C. Stone, "Elemental Composition of the Anomalous Cosmic-Ray Component," *Proceedings of the 20th International Cosmic Ray Conference, Moscow, USSR* 3, 413 (1987).

Cummings, A. C., E. C. Stone, F. B. McDonald, W. R. Webber, and N. Lal, "Radial and Latitudinal Gradients of Anomalous Cosmic-Ray Oxygen and Helium and Galactic Cosmic Rays in the Outer Heliosphere," *Proceedings of the 20th International Cosmic Ray Conference, Moscow, USSR* 3, 417 (1987).

Cummings, A. C. and E. C. Stone, "Energy Spectra of Anomalous Cosmic-Ray Oxygen During 1977-1987," *Proceedings of the 20th International Cosmic Ray Conference, Moscow, USSR* 3, 421 (1987).

Cummings, A. C., R. A. Mewaldt, and E. C. Stone, "Large-Scale Radial Gradient of Anomalous Cosmic-Ray Oxygen from 1 to ~ 30 AU," *Proceedings of the 20th International Cosmic Ray Conference, Moscow, USSR* 3, 425 (1987).

Cummings, A. C., E. C. Stone, and W. R. Webber, "Latitudinal and Radial Gradients of Anomalous and Galactic Cosmic Rays in the Outer Heliosphere," *Geophys. Res. Letters* 14, 174 (1987).

Finger, M. H. and T. A. Prince, "The Source Confusion and Background Fluctuation Limit to the Sensitivity of Low Energy Gamma-Ray Telescopes," *Bull. of Am. Phys. Soc.* 31, 883 (1986).

Garrard, T. L., P. S. Gibner, M. H. Israel, J. Klarmann, C. J. Waddington, and W. R. Binns, "Anisotropy of Galactic Iron of Energy 30 to 500 GeV/amu Studied by HEAO-3," *Proceedings of the 20th International Cosmic Ray Conference, Moscow, USSR* 1, 348 (1987).

Green, M. A., G. F. Smoot, R. L. Golden, M. H. Israel, R. Kephart, R. Niemann, R. A. Mewaldt, J. F. Ormes, P. Spillantini, and M. E. Wiedenbeck, "ASTROMAG: A Superconducting Particle Astrophysics Magnet Facility for the Space Station," *IEEE Trans. on Magnetics* 23, 1240 (1987).

Israel, M. H., M. D. Jones, M. P. Kamionkowski, J. Klarmann, E. C. Stone, C. J. Waddington, W. R. Binns, and T. L. Garrard, "Cosmic-Ray Energy Spectra Between Ten and Several Hundred GeV/amu for Elements from $_{18}$Ar to $_{28}$Ni--Results from HEAO-3," *Proceedings of the 20th International Cosmic Ray Conference, Moscow, USSR* 1, 330 (1987).

Kertzman, M. P., J. Klarmann, B. J. Newport, E. C. Stone, C. J. Waddington, W. R. Binns, and T. L. Garrard, "Fragmentation Cross Sections of Ultraheavy Nuclei," *Bull. of Am. Phys. Soc.* 31, 871 (1986).

Klarmann, J., C. J. Waddington, W. R. Binns, T. L. Garrard, P. S. Gibner, and M. H. Israel, "Response of Ionization Chambers and Cerenkov Counters to Relativistic Ultraheavy Nuclei," *Proceedings of the 20th International Cosmic Ray Conference, Moscow, USSR* 2, 390 (1987).

Klarmann, J., C. J. Waddington, W. R. Binns, T. L. Garrard, P. S. Gibner, and M. H. Israel, "Response of Ionization Chambers and Cherenkov Counters to Relativistic Ultraheavy Nuclei," *Proceedings of 20th International Cosmic Ray Conference, Moscow, USSR* (1987).

Mewaldt, R. A., "^{3}He in Galactic Cosmic Rays," *Ap. J.* 311, 979 (1986).

Mewaldt, R. A. and E. C. Stone, "Solar Coronal Isotopic Abundances Derived From Solar Energetic Particle Measurements ," *EOS Trans. AGU Nov.* 67, 1142 (1986).

Mewaldt, R. A. and E. C. Stone, "Isotopic Abundances of Solar Coronal Material Derived from Solar Energetic Particle Measurements," *Bull. of the Amer. Astron. Soc.* 18, 1042 (1986).

Mewaldt, R. A., "Galactic Cosmic Ray Isotope Spectroscopy: Status and Future Prospects," *Proceedings of the 13th Texas Symposium on Relativistic Astrophysics*, p. 573, World Scientific (1987).

Mewaldt, R. A. and E. C. Stone, "Isotope Abundances of Solar Coronal Material Derived from Solar Energetic Particle Measurements ," *Proceedings of the 20th International Cosmic Ray Conference, Moscow, USSR* 3, 255 (1987).

Newport, B., "The Abundances of Ultraheavy Elements in the Cosmic Radiation," Ph.D. Thesis, California Institute of Technology (1986).

Newport, B. J., E. C. Stone, C. J. Waddington, W. R. Binns, T. L. Garrard, M. H. Israel, and J. Klarmann, "Elemental Abundances of Ultraheavy Cosmic Rays Measured on HEAO-3," *Bull. of Am. Phys. Soc.* 31, 871 (1986).

Ormes, J. F., M. Israel, M. Wiedenbeck, and R. A. Mewaldt, Editors, "ASTROMAG: The Particle Astrophysics Magnet Facility," Interim Report of the Astromag Definition Team (1986).

Ormes, J. F., M. H. Israel, R. A. Mewaldt, and M. Wiedenbeck, "A Particle Astrophysics Magnet Spectrometer Facility for Space Station," *Proceedings of the 20th International Cosmic Ray Conference, Moscow, USSR* **2**, 378 (1987).

Palmer, D. and T. A. Prince, "A Demonstration of Fourier Transform Imaging at Gamma Ray Energies," *Bull. of Am. Phys. Soc.* **31**, 883 (1986).

Palmer, D. and T. A. Prince, "A Laboratory Demonstration of High-Resolution Hard X-ray and Gamma-ray Imaging using Fourier-Transform Techniques," *IEEE Trans. on Nuclear Science* NS-**34**, 71 (1987).

Palmer, D. and T. A. Prince, "A Laboratory Demonstration of High-Resolution Hard X-ray and Gamma-ray Imaging using Fourier-Transform Techniques," *Proceedings of 20th International Cosmic Ray Conference, Moscow, USSR* **4**, 375 (1987).

Stone, E. C., S. P. Christon, and J. T. Hoeksema, "Latitudinal Variation of Cosmic Ray Flux and its Association With the Tilt of the Heliospheric Current Sheet," *EOS Trans. AGU April* **67**, 329 (1986).

Stone, E. C., "An Overview of the Voyager 2 Encounter with Uranus," Invited talk at the COSPAR XXVI Plenary Meeting, Toulouse, France (1986).

Stone, E. C., "The Voyager 2 Encounter with Uranus," *Bull. of the Amer. Astron. Soc.* **18**, 1006 (1986).

Stone, E. C., "An Overview of the Voyager 2 Encounter with Uranus," *EOS Trans. AGU* **67**, 298 (1986).

Stone, E. C. and E. D. Miner, "The Voyager 2 Encounter with the Uranian System," *Science* **233**, 39 (1986).

Stone, E. C., C. J. Waddington, W. R. Binns, T. L. Garrard, P. S. Gibner, M. H. Israel, M. P. Kertzman, J. Klarmann, and B. J. Newport, "The Abundances of Ultraheavy Elements in the Cosmic Radiation," *Proceedings of the 20th International Cosmic Ray Conference, Moscow, USSR* **1**, 366 (1987).

Waddington, C. J., W. R. Binns, T. L. Garrard, M. H. Israel, M. P. Kertzman, J. Klarmann, and E. C. Stone, "Release of Nuclei from Relativistic Nucleus-Nucleus Interactions," *Proceedings of the 20th International Cosmic Ray Conference, Moscow, USSR* **2**, 152 (1987).

Waddington, C. J., W. R. Binns, J. R. Cummings, T. L. Garrard, P. S. Gibner, M. H. Israel, M. P. Kertzman, and J. Klarmann, "The Energy Dependence of Fragmentation Cross-Sections of Relativistic Heavy Nuclei," *Proceedings of the 20th International Cosmic Ray Conference, Moscow, USSR* **2**, 149 (1987).

Webber, W. R., R. L. Golden, and R. A. Mewaldt, "A Re-Examination of the Cosmic Ray Helium Spectrum and the ^{3}He/^{4}He Ratio at High Energies," *Ap.J.* **312**, 178 (1987).